15th International Plansee Seminar, Eds. G. Kneringer, P. Rödhammer and H. Wildner, Plansee Holding AG, Reutte (2001), Vol. 4

A COMPARISON OF THE MICROSTRUCTURE AND HIGH TEMPERATURE TENSILE PROPERTIES OF A NOVEL P/M Mo-Hf-Zr-Ta-C ALLOY AND TZM

J. Warren[⊗] and G. Reznikov*
GE Medical Systems
Coolidge Laboratory, 4855 W. Electric Avenue, W. Milwaukee, WI 53219
*X-Ray Tube Target Plant, 18683 South Miles Road, Warrensville Heights, OH 44128

Abstract

The microstructure and elevated temperature quasi-static tensile yield and ultimate strength observed in a novel, forged Mo-based alloy (Mo-0.25Hf-0.25Zr-0.25Ta-0.025C) has been analyzed and compared to a standard forged TZM composition (Mo-0.50Ti-0.08Zr-0.02C). The novel material exhibits the desirable forging characteristics typical of the widely used TZM composition yet possess a higher ultimate strength and 0.2% offset yield strength in both the stress-relieved and recrystallized conditions over a 400°-1200°C temperature range. The greater strength measured in the novel composition has been attributed to the combined effects of precipitation of Hf, Zr and Mo-(carbide) precipitates that strengthen the matrix in the classical Orowan fashion and improved resistance to recrystallization after high temperature exposure. Elevated temperature creep behavior, not addressed in the study presented here, will be reported on in a subsequent analysis.

Introduction

The development of precipitation strengthened molybdenum alloys such as MHC (Mo-1.0Hf-0.10C), TZC (Mo-1.25Ti-0.15Zr-0.02C) and TZM (Mo-0.5Ti-0.08Zr-0.025C) have resulted in alloys that exhibit outstanding high temperature tensile strength and creep resistance. These alloy derive high temperature strength from a combination of mechanisms which include (1) the precipitation and dispersion of discrete carbide and oxide particles, (2) the retention of a heavily worked molybdenum matrix and (3) solid solution strengthening. Of the three alloy systems described above, TZM has gained the widest commercial acceptance due principally to this alloys relative ease of manufacture into wrought product forms. For ease of fabrication however,

15th International Plansee Seminar, Eds. G. Kneringer, P. Rödhammer and H. Wildner, Plansee Holding AG, Reutte (2001), Vol. 4

a compromise in both elevated temperature strength and resistance to recrystallization at temperature extremes are realized.

This paper describes a novel powder metallurgical alloy system designated Alloy-2 with a nominal composition of Mo-0.25Hf-0.25Zr-0.25Ta-0.03C [1]. This particular composition was down-selected from a larger group of alloys fabricated within the constraints of an experimental design matrix; the goal of which was the development of an alloy that both possessed the favorable hot fabrication characteristics associated with the TZM composition and simultaneously exhibited a significant improvement in elevated temperature strength when compared to the TZM composition processed under identical conditions. Concentrations of the alloying agents hafnium and zirconium (carbide and oxide formers, respectively), tantalum (solid solution strengthener) and carbon where systematically adjusted within the master mix, blended with pure molybdenum powder, pressed and forged into flat disks for subsequent mechanical analysis. Based on the hot yield and ultimate tensile strength data accumulated for all of the compositional variations investigated in the experimental matrix, the material analyzed in this report, Alloy-2, was selected as a promising candidate for continued evaluation.

Manufacturing cost is a significant consideration in the industrial setting and improvements in elevated temperature mechanical behavior must be assessed against both an alloys ease of fabrication and the potential advances in components manufactured from the alloy, especially with the added expenses associated with alloying agents rich in hafnium and tantalum. For example, in the manufacture of high power TZM rotating anode x-ray tube targets, the elevated temperature yield and creep resistance of TZM restricts the size and rotational speed of the hot target thus limiting useful x-ray output power. Higher hot strength target alloys that incur greater fabrication costs enable greater x-ray power output which, from the customers perspective, adds value that justifies the premium paid.

In this report, the elevated temperature yield and ultimate strength comparisons between Alloy-2 and TZM are made. Each alloy system was tested in two heat-treated conditions; a partially recrystallized condition denoted in this report as *stress relieved* and fully *recrystallized*. Recrystallization is especially of interest since the thermal processing normally associated with x-ray tube target manufacture (i.e. brazing and

15th International Plansee Seminar, Eds. G. Kneringer, P. Rödhammer and H. Wildner, Plansee Holding AG, Reutte (2001), Vol. 4

vacuum degassing) usually results in a target alloy that is placed in service in a condition that has undergone recrystallization and grain growth.

Materials

Rectangular tensile test specimen blanks of both the TZM (Mo-0.5Ti-0.08Zr-0.03C) and Alloy-2 (Mo-0.25Hf-0.25Zr-0.25Ta-0.03C) compositions were wire EDM cut from forged target disks 185mm in diameter and 18mm thick as shown in Fig. 1. The disks for this study were manufactured at the GE X-ray Tube Target Plant (Warrensville Heights, OH) and processed using parameters suited for the fabrication of molybdenum based x-ray tube target assemblies. Unlike monolithic wrought molybdenum alloys, x-ray tube targets are pressed and forged with an integral tungsten-rhenium (W-Re) outer annulus (i.e. *track*) about 1mm thick which serves as the focal spot for electron beam impingement and subsequent x-ray generation. Thus, the presence of the track in contact with the substrate, must be accounted for during processing. Theoretically, to achieve the highest possible strength, a solution heat treatment that effectively dissolves preexisting carbide inclusions and homogenizes the alloying elements within the matrix for subsequent controlled precipitation by aging is necessary. For example, solution treatment temperatures greater than 2300°C followed by rapid furnace cooling favor the kinetics of complete dissolution of the (Zr, Ti)C and Mo_2C carbides in TZM. This heat treatment would then be followed by controlled aging, elevated temperature forging and final stress relieving at temperatures typically between 1100°-1200°C. However, to avoid the deleterious diffusion affects (Kirkendall porosity) associated with the W-Re track in contact with the molybdenum substrate at temperatures greater than 2300°C, sintering temperatures are limited in this production program to 2000°-2100°C; a temperature range where the kinetics of grain boundary Mo_2C formation is favored [2].

15th International Plansee Seminar, Eds. G. Kneringer, P. Rödhammer and H. Wildner, Plansee Holding AG, Reutte (2001), Vol. 4

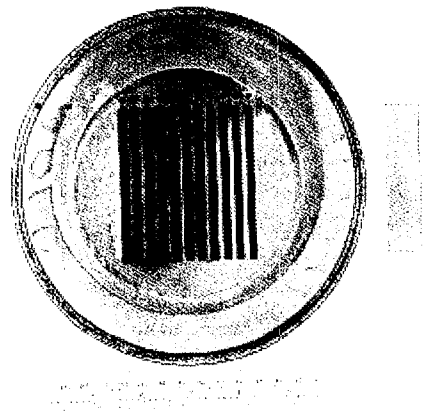

Figure 1. Method of specimen removal from a test forging.

The standard processing route used at GE for the production of TZM x-ray targets was used for the fabrication of the samples manufactured from the Alloy-2 material. The process begins by first cold pressing blended powder compositions of each alloy to a green density of approximately 0.65 theoretical. The density is further increased to nearly 0.95 theoretical by vacuum or hydrogen sintering between 2000° and 2100°. Using the same die and identical forging parameters, the sintered targets are preheated to 1500°-1550°C and subsequently hot forged. A moderate reduction in the through thickness of about 20% is achieved during forging resulting in a final density of about 0.99 theoretical for both the TZM and the Alloy-2 substrates. As discussed previously, stress relieving is accomplished at a relatively high temperature; 1500°-1550°C for 30 minutes in a dry hydrogen batch furnace. The forgings exit the hot-zone and are immediately cooled by convection in a hydrogen purged cold-zone outfitted with water-cooled muffles. In addition to having cooling rates faster than those obtained by air cooling, hydrogen cooling results in part surfaces that are oxide free. After deformation processing, the carbon content in each alloy was measured to be approximately 300-600 ppm by wt. Residual oxygen content is typically less than 30 ppm by weight for both alloy compositions.

Two separate heat treatments of each alloy were tensile tested between 400° and 1200°C. First, tensile specimens were extracted from forgings in the stress relieved condition. Second, in order to investigate and compare the

15th International Plansee Seminar, Eds. G. Kneringer, P. Rödhammer and H. Wildner, Plansee Holding AG, Reutte (2001), Vol. 4

effect of heat treatment on the structure and properties, the target disks were exposed to an extensive recrystallization vacuum heat treatment at 1900°C for 3h. Tensile specimens were then machined (EDM) from these target disks, tensile tested and compared. Specimens were removed from the target disk centers (see Fig. 1) far removed from the influence of the W-Re track located at the outer edge.

The microstructures of each alloy composition were studied using optical, SEM and TEM methods. EDS was used to acquire chemical composition data for the precipitates observed (both the SEM and TEM used in this investigation had this capability). In Fig. 2a and b, SEM photomicrographs of the TZM and Alloy-2 compositions respectively, exposed to the stress relieving heat treatment, are shown and compared. The microstructures shown are views which are normal to the through-thickness of the disk. Average grain sizes, measured using the Hilliard circle technique, were found to be similar at 22μm for the TZM alloy and 27μm for Alloy-2. Conventional, stress relieved TZM wrought product, subjected to extensive forging or hot extrusion processing will have grain sizes finer than the ones measured here. Also, the relatively high temperature stress relieving temperature used in this study results in recovery and partial recrystallization of the matrix.

In the stress relieved TZM composition two distinct precipitates were observed. SEM analysis revealed large Mo and Ti carbide precipitates, $Mo_2(Ti)C$, located both in grain interiors and along grain boundaries while TEM analysis revealed an extremely fine (<50nm) Zr oxide, ZrO_2, precipitate array located within the grain interiors. Based on the size and large separation distances of the carbide precipitates revealed in the TZM microstructure it is reasonable to assume that they do not contribute to strengthening in the classical fashion. An example of the two precipitate morphologies can be seen in the TEM micrograph shown in Fig. 3 where the small arrows highlight the extremely fine ZrO_2 precipitate array and the large arrows locate a typical grain boundary carbide.

15th International Plansee Seminar, Eds. G. Kneringer, P. Rödhammer and H. Wildner, Plansee Holding AG, Reutte (2001), Vol. 4

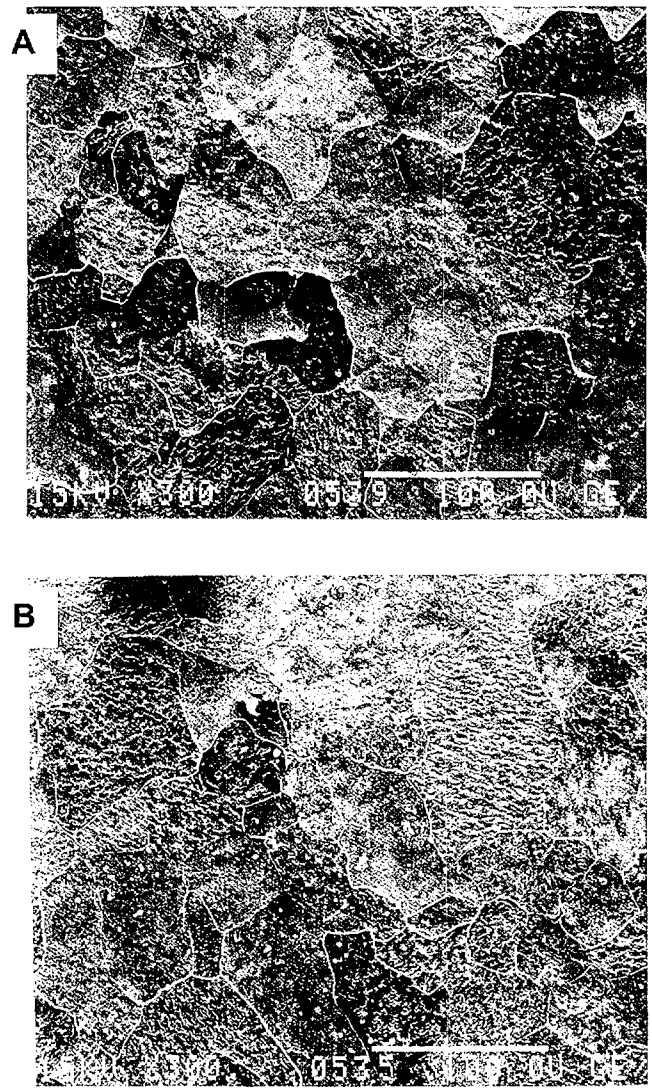

Figure 2. Microstructure of A) TZM and B) Alloy-2 in stress-relieved condition.

By comparison, the stress relieved Alloy-2 composition possessed two precipitate types. Large oxide precipitates of Hf and Zr located within the grains and a much finer distribution of Hf, Zr and Mo-rich precipitates inside the grains with a size distribution ranging from approximately 30nm to about

15th International Plansee Seminar, Eds. G. Kneringer, P. Rödhammer and H. Wildner, Plansee Holding AG, Reutte (2001), Vol. 4

1μm with a separation distance which appears to be significantly smaller than the corresponding ZrO_2 precipitate spacing observed in the TZM alloy. EDS spectra taken from these particles over the range of sizes observed were nearly identical suggesting that the extremely small precipitates are nuclei of the larger precipitates. Diffraction patterns were taken from these precipitates but, at the time of this writing, the analysis could not accurately determine their structure. Diffraction patterns typical of the MC structure were not observed. EDS spectra did not reveal the presence of oxygen hence the form is likely that of a carbide. A TEM micrograph of the material, Fig. 4, shows how these (carbide) precipitates, especially the extremely fine ones, are arranged in the matrix. The (carbide) precipitates are highlighted by the arrows. Also, the grain boundary shown in Fig. 4 is free of large precipitates and typifies the grain boundaries in this composition. Grain boundary precipitates were not observed in this composition. The (carbide) precipitates can be seen in the SEM photomicrograph shown in Fig. 2b (see arrows). As is evident from the figure, the precipitate density appears to vary significantly from grain to grain.

Higher magnification TEM micrographs are shown in Figures 5 and 6 and illustrate the extent of retained hot work in the TZM and Alloy-2 matrices due to forging and subsequent stress relieving, respectively. Both figures show a typical dislocation arrangement. Close examination of Fig. 5 also shows clearly that the extremely fine ZrO_2 precipitates interact and impede dislocation slip generated during forging. The comparison (Fig. 6A and B) also reveals that Alloy-2 appears to contain a significantly higher number of dislocations than the TZM composition with many of the Alloy-2 grains containing a refined cell structure (6B) with some grains possessing a roughly equiaxed cell morphology.

15th International Plansee Seminar, Eds. G. Kneringer, P. Rödhammer and H. Wildner, Plansee Holding AG, Reutte (2001), Vol. 4

Figure 3. Large arrow indicates typical grain boundary carbide in stress-relieved TZM and the small arrows show typical matrix precipitate morphology.

15th International Plansee Seminar, Eds. G. Kneringer, P. Rödhammer and H. Wildner, Plansee Holding AG, Reutte (2001), Vol. 4

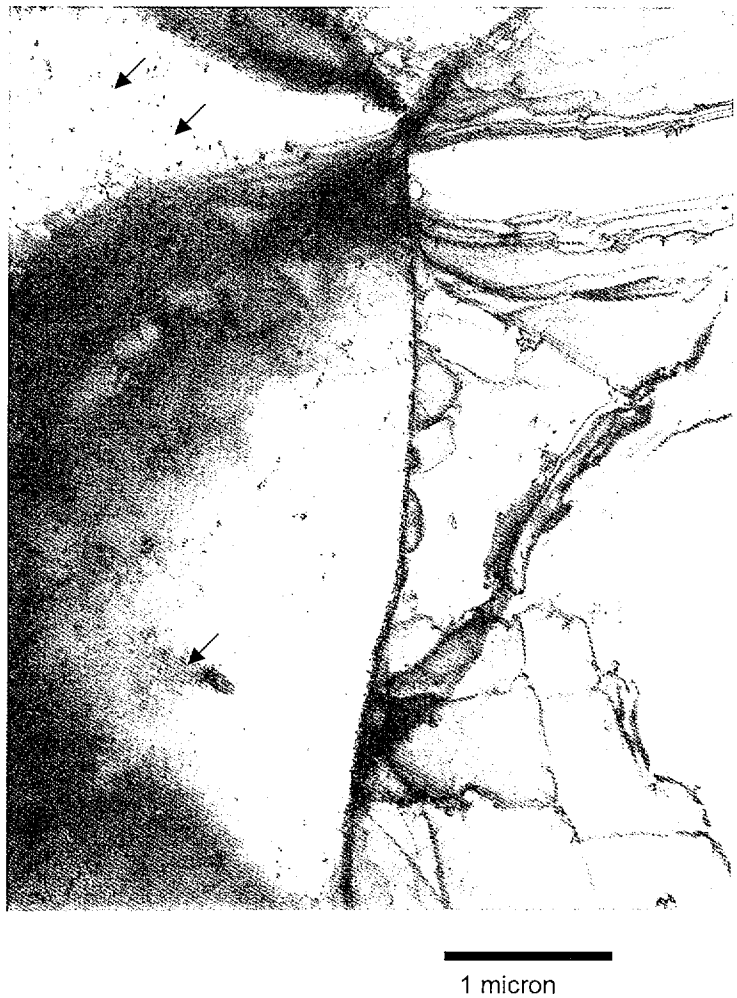

Figure 4. Arrows highlight precipitates in stress-relieved Alloy-2.

Recrystallizing each alloy results in significant changes in the microstructure. As expected the average grain sizes increased. For example, the TZM alloy increased to 48μm while for the Alloy-2 composition a value of 44μm was measured which indicates that the grain growth kinetics are similar between the two alloy systems. TEM analysis of each alloy also indicated that the ZrO_2 in the stress relieved TZM and the Hf, Zr, and Mo-(carbide) precipitates in the stress relieved Alloy-2 coarsened to some extent as a result of the heat

15th International Plansee Seminar, Eds. G. Kneringer, P. Rödhammer and H. Wildner, Plansee Holding AG, Reutte (2001), Vol. 4

treatment with a corresponding decrease in the separation distance between particles.

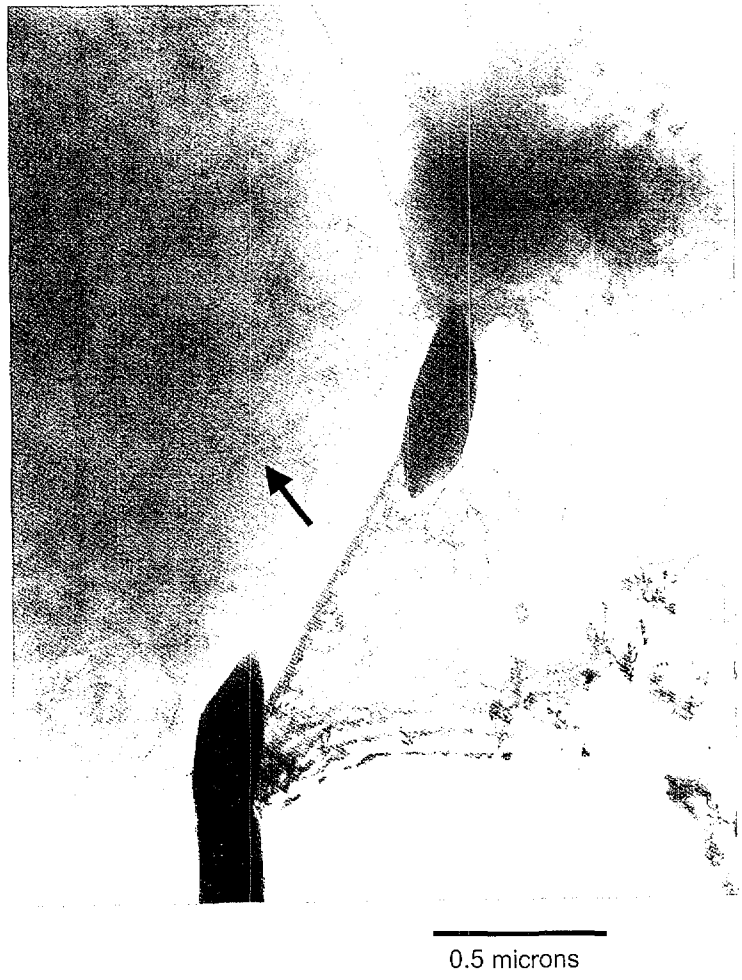

Figure 5. Arrow highlights dislocation interactions with matrix precipitates.

15th International Plansee Seminar, Eds. G. Kneringer, P. Rödhammer and H. Wildner, Plansee Holding AG, Reutte (2001), Vol. 4

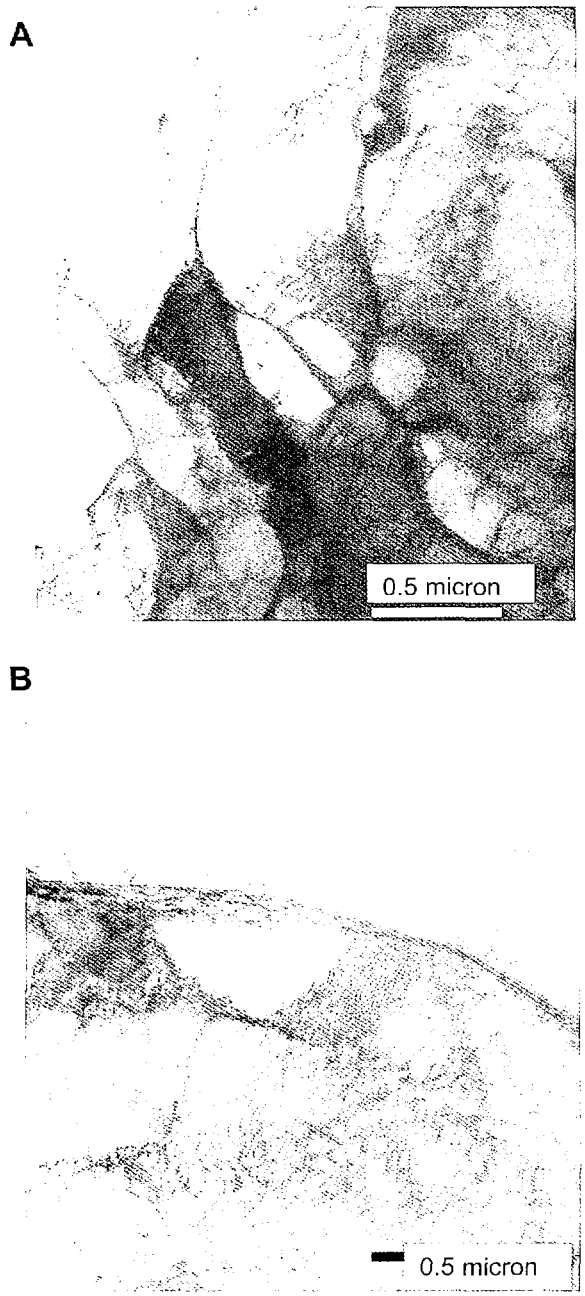

Figure 6. Alloy 2: A) dislocation density B) refined cell structure

15th International Plansee Seminar, Eds. G. Kneringer, P. Rödhammer and H. Wildner, Plansee Holding AG, Reutte (2001), Vol. 4

Tensile Testing Procedure

Pin-loaded tensile specimens per ASTM E21-92 were cut from both the stress relieved and the recrystallized TZM and Alloy-2 forgings as shown in Fig. 7. Gage extension was measured using a direct contact extensometer. To maintain a constant tensile strain-rate in the gage, the output signal from the extensometer was used to control the cross-head velocity using a PC interface. All tests were conducted with a constant gage strain-rate of 8.3×10^{-5}/sec. After reaching approximately 1% strain, the test was switched to a constant cross-head velocity test of 0.02mm/sec (8.3×10^{-4}in./sec). All tensile tests were conducted to rupture.

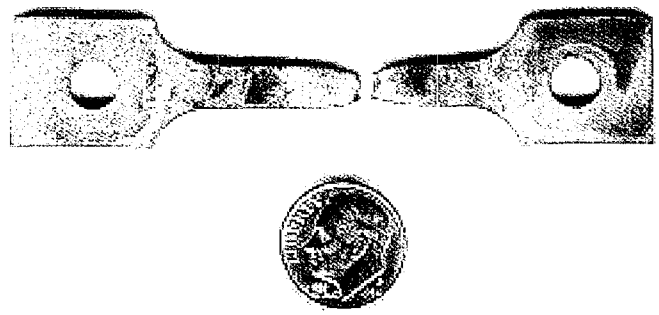

Figure 7. A typical tensile rupture.

Tensile tests were conducted in a two-zone furnace "clam-shell" type furnace purged with a constant flow of high pressure nitrogen gas for all test temperatures up to and including 1000°C. Argon gas flow was then used at the highest test temperature, 1200°C. Tension tests were conducted at 400°, 600°, 800°, 1000° and 1200°C. Prior to load application, specimens were soaked for 30 minutes at each temperature. Outputs from the extensometer and load cell were sent to a data logging PC. Engineering stress-strain curves were then determined from the recorded data. Three tensile tests (replicates) were conducted at each test temperature listed above. From the stress-strain plots the 0.002 offset yield strength was established for each alloy and associated heat treatment. The average strength is reported.

15th International Plansee Seminar, Eds. G. Kneringer, P. Rödhammer and H. Wildner, Plansee Holding AG, Reutte (2001), Vol. 4

Results and Discussion

The tensile testing results of the two compositions exposed to the stress relieving heat treatment are shown in Fig. 8 where the average offset yield strength at 0.002 (0.2%) engineering strain is plotted against the test temperature range of 400°-1200°C. As is evident in the Fig. 8, the yield strength of Alloy-2 is approximately 100MPa higher than the values measured in the TZM material over the entire test temperature range. From a qualitative standpoint, a higher yield strength in Alloy-2 is expected based on the observation of the refined dislocation substructure retained after stress relieving as shown in Fig. 5. A comparison of average ultimate tensile strength (UTS) data, Fig. 9, clearly indicates a higher strain hardening coefficient associated with Alloy-2 resulting in a greater dislocation density and corresponding flow stress for a given strain increment. Based on this observation, it is reasonable to assume that the precipitate density in Alloy-2 is higher than TZM. Examination of Fig. 8 also shows that the yielding is somewhat insensitive to the test temperature and explanations in terms of precipitation strengthening and dynamic strain aging (DSA) are considered. For example, each alloy system relies primarily on the dispersion of hard incoherent precipitates to strengthen the matrix by both stabilizing a finer substructure during the forging operation and by blocking dislocations during plastic deformation in the classical Orowan fashion. In the case of the TZM composition fabricated for this study, the precipitates consist primarily of the very large grain boundary $Mo_2(Ti)C$ type and extremely fine ZrO_2 precipitates observed in the molybdenum matrix. In this analysis it is assumed that the principle strengthening of the TZM matrix is associated with the Zr oxide precipitate array. By comparison, particle strengthening in Alloy-2 is derived from the Hf, Zr, and Mo-(carbide) precipitates. Hence the observed differences in 0.2% offset tensile yield strength observed between the two alloy compositions can be analyzed based on the incremental tensile strength increase, $\Delta\sigma$, associated with the presence (or absence) of matrix precipitates and the associated dislocation blocking mechanism.

15th International Plansee Seminar, Eds. G. Kneringer, P. Rödhammer and H. Wildner, Plansee Holding AG, Reutte (2001), Vol. 4

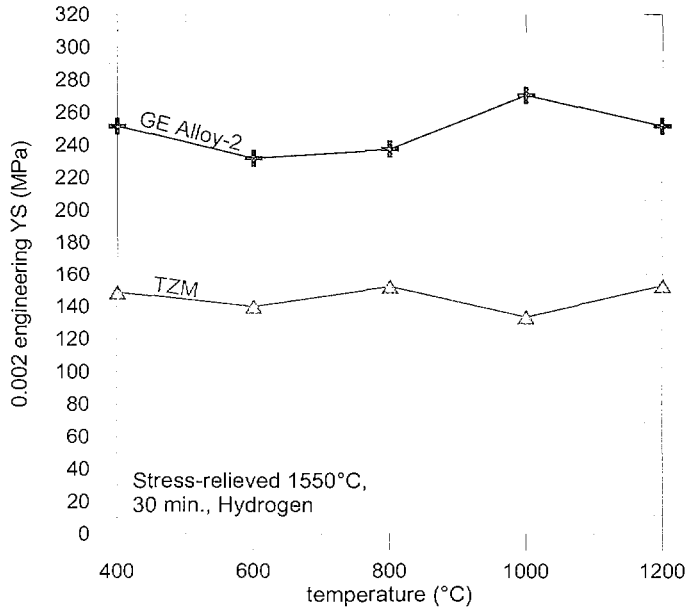

Figure 8. Yield strength of TZM and Alloy 2 after 1550°C heat treatment.

Both long-range and short-range interactions contribute to strengthening. The long range interactions arise from the internal elastic strain fields associated with the presence of the precipitates and the resultant interaction of dislocations with the distorted matrix. Short range interactions however, contribute to the majority of the strengthening seen in these alloys [3]. The tensile yield stress increment associated with short range strengthening has been calculated by Orowan and is approximately equal to:

$$\Delta\sigma \sim 4G\mathbf{b}/L$$

where G is the temperature dependent shear modulus of the Mo-matrix, **b** is the Burgers vector of the Mo-matrix ($2.73X10^{-10}$ m) and L is the particle to particle separation distance. A quantitative analysis of the density of extremely fine precipitates present in each alloy composition was not made for this study. If however, the assumption is made that the extremely fine precipitates in each alloy strengthen the Mo-matrix in a similar fashion the higher strength associated with Alloy-2 can, in part, be attributed to the presence of the dispersion of the somewhat coarser Hf, Zr, and Mo-(carbide) precipitates observed under the SEM (see arrows in Fig. 2b). For example, the estimated particle to particle separation distance of these precipitates in Alloy-2 is about 4μm which, based on the Orowan relationship, corresponds

15th International Plansee Seminar, Eds. G. Kneringer, P. Rödhammer and H. Wildner, Plansee Holding AG, Reutte (2001), Vol. 4

to an incremental strength increase of about 34MPa at 400°C. Hence, Orowan strengthening, in conjunction with higher resistance to recrystallization, likely accounts for the greater offset yield strength observed with the stress-relieved Alloy-2 composition.

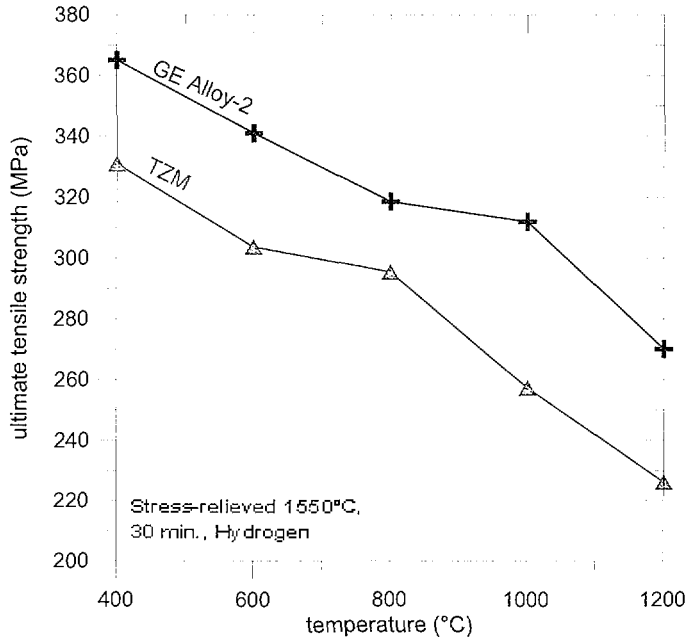

Figure 9. Ultimate strength after 1550°C heat treatment

15th International Plansee Seminar, Eds. G. Kneringer, P. Rödhammer and H. Wildner, Plansee Holding AG, Reutte (2001), Vol. 4

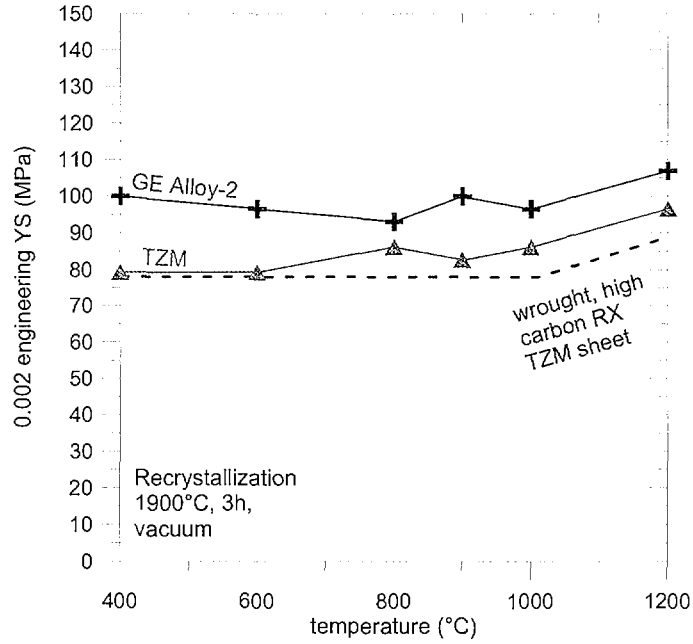

Figure 10. Yield Strength after 1900°C heat treatment

The shear modulus of Mo at 400°C is about 94% of the value at 25°C while at 1200°C it reduces to approximately 83%. With the exception of the matrix shear modulus, the remaining physical parameters of the Orowan relationship are independent of temperature. Based on this analysis, if the Orowan mechanism was the only mechanism active in each alloy, a relatively small (~12%) reduction in strength would be observed between the two test temperature extremes. Counteracting the reduction in strength associated with increasing temperature is the anomalous hardening behavior observed in dispersion strengthened BCC alloys due to the interaction of dislocations with solutes (i.e. DSA) [2]. The DSA strengthening mechanism is likely active in the stress relieved compositions and clearly apparent in the recrystallized alloy compositions, Fig. 10, where the average 0.2% yield stress is plotted over the test temperature range. As is shown in Fig. 10, the yield stress of both alloys increases gradually above about 1000°C. Based on the classical interpretation of DSA, the drag stress imposed on mobile dislocations increases as the mobility of solutes within the lattice increases resulting in a gradual increase in strength. A number of investigations have shown that the

15th International Plansee Seminar, Eds. G. Kneringer, P. Rödhammer and H. Wildner, Plansee Holding AG, Reutte (2001), Vol. 4

activation enthalpy of DSA is the same as interstitial diffusion [2]. The temperature range where DSA is active in Mo-based alloys is between about 800° and 1200°C and is readily observed in Mo-based alloys that retain a significant fraction of alloying elements in solution, i.e. quenched from a recrystallization heat treatment. DSA is also observed in recrystallized TZM that is furnace cooled which suggests that the precipitation kinetics associated with TZM are sufficiently slow enough to retain a reasonable fraction of solutes in the matrix. Hence, it is reasonable to assume that DSA is active in both recrystallized alloy compositions and can explain the increase in strength shown in Fig. 10 above 1000°C.

As expected, comparison of Fig. 10 to Fig. 8 shows that recrystallizing the stress relieved alloys reduces the yield strength of each composition dramatically. TZM exhibits approximately a 70MPa average reduction while the Alloy-2 composition drops nearly 150MPa; a difference of 80MPa. Grain growth, particle coarsening and a reduction in the dislocation density associated with hot working are the principle factors that contribute to the drop in strength. Of particular interest is the larger drop in strength observed in Alloy-2 likely a result of a significantly greater reduction in the dislocation density than that which occurs in the TZM composition.

The role of the tantalum addition and its contribution to strengthening, if any, was not investigated in this report. No precipitates containing tantalum were observed and, based on EDS analysis of the matrix, it appears to be present entirely in solution

Conclusions

In summary, the strength observed in the Alloy-2 material has been attributed to the
presence of a fine distribution of Hf, Zr, and Mo-(carbide) precipitates that strengthen
the material in the classical Orowan fashion. The strength of this alloy is significantly higher than TZM after thermal exposures to temperatures as high as 1550°C yet possess similar forging and machining characteristics. Modifications to this novel alloy are planned and include an analysis designed to study the effect varying the weight fraction of tantalum has on strength.

15th International Plansee Seminar, Eds. G. Kneringer, P. Rödhammer and H. Wildner, Plansee Holding AG, Reutte (2001), Vol. 4

References

1. US Patent No. 5222116; Metallic Alloy for X-ray Target (1992)
2. E. Pink, A Review of Deformation Mechanisms in Particle Strengthened Molybdenum Alloys, *Refractory Metals and Hard Materials*, Dec. 1986, pp. 192-99.
3. A. Lou *et al*, High Temperature Tensile Properties of Molybdenum and a Molybdenum-0.5% Hafnium Carbide Alloy, *Scripta Metallurgica et Materialia*, Vol. 29, 1993, pp. 729-732.